Research Square

Preprints are preliminary reports that have not undergone peer review.
They should not be considered conclusive, used to inform clinical practice,
or referenced by the media as validated information.

Computational Identification and Evaluation of Curcumin Derivatives as Potential Inhibitors of PPP2R5B to Enhance Insulin Sensitivity

Sadaf Mumtaz
Ziauudin University
Maaz Waseem
National University of Sciences and Technology (NUST)
Zainab Kamran
National University of Sciences and Technology (NUST)
Saifullah Khan
National University of Sciences and Technology (NUST)
Maham Yamin
Research Innovation & Commercialization, Rawalpindi Medical University
Aneela Javed
javedaneela19@gmail.com

National University of Sciences and Technology (NUST)

Article

Keywords: Insulin resistance, PPP2R5B, Curcumin derivatives, Molecular docking, Molecular dynamics simulation, Akt signaling

Posted Date: October 23rd, 2025

DOI: https://doi.org/10.21203/rs.3.rs-7415440/v1

License: This work is licensed under a Creative Commons Attribution 4.0 International License. Read Full License

Additional Declarations: No competing interests reported.

Version of Record: A version of this preprint was published at Scientific Reports on April 18th, 2026. See the published version at https://doi.org/10.1038/s41598-026-43433-8.

Abstract

Insulin resistance has been intricately linked to impaired Akt signaling due to the hyperactivation of protein phosphatase 2A (PP2A). Specifically, the regulatory subunit PPP2R5B plays a crucial role in this dysregulation, making it a promising therapeutic target. This study aimed to identify novel curcumin-derived phytochemicals capable of inhibiting PPP2R5B and improving insulin sensitivity. Initially, approximately 85 curcumin-related compounds were retrieved from the PubChem database and subjected to extensive virtual screening via molecular docking. Among these, curcumin-bicyclopentadione emerged as the lead candidate, exhibiting the strongest binding affinity (− 9.2 kcal mol□□) due to its extensive interactions with key residues ARG64, GLN439, and ARG385. Further MD simulations confirmed their robust binding stability, highlighting sustained hydrogen bonds and minimal structural fluctuations. Pharmacokinetic analyses using DeepPK profiling predicted favorable ADMET properties, including minimal toxicity, no significant cytochrome P450 inhibition, and negligible cardiotoxicity risks. These computational predictions suggest that curcumin-bicyclopentadione and closely related derivatives could effectively inhibit PPP2R5B activity, thereby restoring Akt phosphorylation and insulin-mediated glucose uptake. While promising, these findings necessitate subsequent validation through rigorous experimental assays. The integration of computational and experimental methodologies may ultimately facilitate the development of novel curcumin-based interventions for insulin resistance and associated metabolic disorders, expanding the therapeutic utility of phytochemicals in metabolic disease management.

1. INTRODUCTION

The metabolic syndrome is a group of risk factors for diabetes and cardiovascular disease that coexist in one person and include dyslipidemia, hypertension, glucose intolerance, and abdominal obesity. It is characterized by a marked disruption in cellular biochemical processes that convert nutrients into energy. The primary factors contributing to the occurrence of such disorders include genetics and abnormalities in the endocrine system [1]. The incidence of these disorders has rapidly grown on a global scale as a result of changing lifestyles, accelerating economic development, global warming, and population ageing [2, 3]. The two most prevalent and avoidable metabolic diseases are diabetes mellitus and obesity, which can lead to dyslipidemia and hypertension [2]. Obesity has affected people of all age groups and shown a twofold escalation in prevalence over the past three decades [4]. According to World Health Organization, 2.5 billion adults aged 18 years and older were overweight in 2022, including over 890 million adults who were living with obesity (https://www.who.int/news-room/fact-sheets/detail/obesity-and-overweight). Similarly, there is an alarming rise in the prevalence of diabetes mellitus which is a major health burden involving impairment of insulin metabolism [5]. Over the course of time, there has been a significant increase in the prevalence of metabolic

syndrome, reaching a point where it is attaining an epidemic magnitude [6]. Although numerous therapeutic options have been established to combat these illnesses, their incidence and prevalence continue to rise sharply. In Pakistan, the prevalence of metabolic disorders is 18%, inflicting a major strain on the country's economy (7).

In diabetes mellitus and obesity, there is a substantial rise in the amount of serum fatty acids which subsequently increases the activity of protein phosphatase 2A (PP2A) enzyme [7]. This serine/ threonine phosphatase enzyme which influences a variety of biological processes is widely expressed as a holoenzyme and is composed of three subunits: A, B, and C, referred to as the scaffolding, variable regulatory, and catalytic subunits, respectively [8]. Its versatility arises from interaction between core enzyme and regulatory-B subunits, adding to its specific attributes [9]. Furthermore, a number of clinical disorders have been linked to the development and progression of disruptions in signaling pathways controlled by particular PP2A complexes [8]. By adversely affecting the Akt node's function, this enzyme increases insulin resistance [10]. Under normal physiological conditions, insulin stimulates Akt, which in turn inhibits the transcription factor FoxO1, necessary for the activation of gluconeogenic enzymes such as glucose-6-phosphatase and phosphoenolpyruvate carboxykinase [11]. Akt also inhibits transcription factor glycogen synthase kinase (Gsk3α), which is an inhibitor of glycogen synthase enzyme. Thus, PP2A activation negatively influences these pathways and leads to increased gluconeogenesis and decreased glycogen synthesis [7]. Also, inhibition of Akt by PP2A increases insulin resistance by negatively affecting glucose transporter-4 (GLUT-4) membrane translocation, which is promoted by the Akt node [10]. Specifically, serine/threonine-protein phosphatase 2A 56 kDa regulatory subunit beta isoform (PPP2R5B), a regulatory subunit of PP2A, mediates Akt dephosphorylation by facilitating the interaction between Akt and PP2A [12]. A study conducted by M Beg *et al.* revealed that increased PPP2R5B expression leads to diminished insulin signaling [13]. Moreover, in obese individuals adipokine – resistin has been reported to increase the activity of the PP2A enzyme [14]. Hence, therapeutic strategies targeting the PP2A enzyme offer valuable prospects for the effective treatment of different metabolic disorders. The main focus of current medications for metabolic diseases is on particular nutrient metabolism pathways; however, many medications have drawbacks, including low compliance, exorbitant costs, and possible adverse effects (16, 17). Medicinal plants are a promising alternative for treating metabolic illnesses because they contain bioactive substances that are widely accessible, affordable, and have fewer adverse effects (17, 18).

Curcumin is a bioactive phytoconstituent obtained from the medicinal plant turmeric (Curcuma longa) rhizome [15]. It has shown valuable effects in ameliorating chronic inflammatory disorders (20), and improved dyslipidemia [16], high blood sugar [17], and high blood pressure [18], while acting as an antioxidant and anti-obesity agent [19]. Latif *et al.* reported that daily supplementation of turmeric leads to a profound reduction in

body mass index (BMI) and systolic blood pressure in overweight and obese females [20]. A scientific report indicated that curcumin inhibits the activity of PP2A enzyme [21]. Regarding its molecular mechanisms, a study revealed that curcumin modulates the function of PP2A enzyme by binding to its Psr A subunit [22]. These findings suggest that curcumin affects important metabolic pathways and could be a useful treatment for diabetes, hypertension, and obesity.

Through an *in silico* approach, the current work aimed to identify compounds that can potentially target the druggable binding sites of the PP2A protein subunit (serine/threonine-protein phosphatase 2A 56 kDa regulatory subunit beta isoform) in curcumin phytoconstituents. The primary aim of this study was to employ a comprehensive virtual screening strategy that integrates ligand-receptor interactions, molecular docking, and dynamic simulation analyses to identify and assess the potential of bioactive compounds derived from curcumin as serine/threonine-protein phosphatase 2A 56 kDa regulatory subunit beta isoform inhibitors.

2. RESULTS

2.1 Structure retrieval and refinement

We initially retrieved information on the gene '*PPP2R5B*' and its canonical protein-coding sequence, 'Serine/threonine-protein phosphatase 2A 56 kDa regulatory subunit beta isoform,' of *Homo sapiens* from the UniProt database. This protein sequence comprises 497 amino acids, with a molecular weight of 57,393.19 Daltons and a theoretical pI of 6.27. Notably, it contains a higher number of leucine and glutamine residues, 65 and 46, respectively, compared to other amino acids. Tryptophan is the least abundant amino acid, with only five residues present. The total number of negatively charged residues (aspartate and glutamate) is 63, while the positively charged residues (arginine and lysine) total 58. The N-terminal of this protein sequence is methionine (M), and its estimated half-life is 30 hours in mammalian reticulocytes *in vitro*. The aliphatic index of this protein is 93.32, and the grand average of hydropathicity (GRAVY) is -0.278.

The 3D model of the desired protein encoded by the *PPP2R5B* gene was retrieved from SWISS-MODEL. Before further use, the structure was meticulously cleaned to remove any heteroatoms, ions, or other bound molecules. Structural assessments and validations were conducted to ensure the quality of the protein model. Ramachandran plot (Fig. 1) analysis revealed that 93.9% of the protein residues were in the most favored region, and 5.8% in the allowed region. Moreover, based on an investigation of 118 structures with a resolution of at least 2.0 Angstroms and an R-factor of no more than 20%, a good quality model is anticipated to have over 90% in the most favorable regions. The Ramachandran plot confirms the selection of a high-quality model in our study. Subsequently, energy

minimization of the selected protein homology model was performed to determine the optimal molecular arrangement in space.

2.2 Ligand library preparation of the curcumin analogues

Using the keyword "curcumin," we identified approximately 85 compounds from the PubChem database. Applying the default filter parameters and reviewing the available literature, we identified 85 relevant bioactive medicinal compounds (Supplementary Tables S1). All available information was retrieved, and the compound structures were downloaded from the SDF. Subsequently, these SDF files were converted to PDB files using the Discovery studio Visualizer, with set default conditions for hydrogen ion addition at neutral pH. Finally, all the compounds were visually inspected. The analogues were then prepared for molecular docking and converted to PDBQT format using AutoDockTools. As an integral step in the comprehensive drug design process, we conducted energy minimization for all selected compounds. This ensured that the arrangement of atoms achieves a net inter-atomic force close to zero, securing a stable position on the potential energy surface [54].

2.3 Molecular Docking Analysis

Molecular docking was implemented using AutoDock Vina, with grid parameters centered on the Fpocket-predicted basic groove of *PPP2R5B*, as described in the Methodology section. Among the 85 curcumin analogues screened, curcumin bicyclopentadione emerged as the top-scoring ligand with a binding energy of -9.2 kcal mol^{-1} (Fig. 2). Its pose occupied the canonical LxxIxE-recognition cleft and established an extensive polar network with GLN 439, ARG 385, and LYS 441, complemented by hydrophobic contacts with ILE 387 and LEU 388 and additional anchoring to the N-terminal ARG 64 and ARG 63. The simultaneous engagement of both the N- and C-terminal basic patches rationalises its superior affinity. It suggests that the bicyclic scaffold effectively pre-organizes the β-diketone core for optimal hydrogen bonding.

Perfluoro-curcumin ranked second at -8.9 kcal mol^{-1} (Fig. 3). Although it preserved contacts with LYS 94 and LYS 341, the substitution of β-diketone hydrogens by fluorine redirected the ligand slightly away from ARG 385 and GLN 439 and toward a more hydrophobic micro-environment defined by PHE 339 and SER 283. This shift reduced the number of strong hydrogen bonds and explains the 0.3 kcal mol^{-1} drop in predicted free energy relative to the bicyclopentadione analogue, despite favourable van-der-Waals contributions from the fluorinated ring.

The remaining four hits displayed progressively weaker scores (Table 1). Curcumin 4′-O-β-D-gentiobioside (–8.4 kcal mol^{-1}) and the diglucoside (–8.2 kcal mol^{-1}) still engaged core

residues such as GLN 439, ARG 385, and ILE 437 but projected bulky sugar chains toward solvent, incurring an entropic penalty that counterbalanced their extensive hydrogen-bonding capacity. The methoxy-benzylidene derivative (–8.3 kcal mol⁻¹) retained the key ARG 64-ARG 385-GLN 439 triad yet lacked the additional hydrophobic clamp contributed by LEU 388, while curcumin-β-D-glucuronide sodium salt (–8.0 kcal mol⁻¹) bound peripherally, interacting mainly with ILE 27, LYS 383 and ARG 385 and burying a smaller fraction of its surface area inside the pocket.

Taken together, the docking results indicate that high-affinity binding requires simultaneous polar contacts with ARG 64 (N-terminal helix) and the C-terminal cluster centred on ARG 385, GLN 439 and LYS 441, reinforced by hydrophobic packing against LEU 388 and ILE 437. Compounds that satisfy this dual-anchor criterion, most notably curcumin bicyclopentadione, therefore constitute promising lead scaffolds for experimental validation as allosteric inhibitors of *PPP2R5B*.

Table 1

Selected Curcumin compounds. This table presents the top six phytochemicals from docking analysis, corresponding to the compound names, binding scores, and interacting residues, highlighting their potential in modulating PPP2R5B.

Compounds	Binding Energy	Interacting Residues
Curcumin_Bicyclopentadione	-9.2	GLN A:439, ARG A:385, LYS A:441, ILE A:387, LEU A:388, ASN A:381,ARG A:64,A:63
perfluoro_curcumin	-8.9	SER A:283, LYS A:94, LYS A:341, PHE A:339, ASP A:193, ASN A:177, THR A:226, SER A:285
curcumin_4'_O_beta_D_gentiobioside	-8.4	ALA A:386, GLN A:439, LEU A:435, VAL A:49, A:69, TYR A:67
4-(4-Hydroxy-3-methoxybenzylidene)-1,7-bis(4-hydroxy-3-methoxyphenyl)hepta-1,6-diene-3,5-dione	-8.3	ARG A:64, GLN A:439, ARG A:385, ALA A:386, TYR A:67, ILE A:437
Curcumin_diglucoside	-8.2	ILE A:437, TYR A:67, TYR A:436, PHE A:51, VAL A:69, HIS A:18, ARG A:379, ASN A:433
Curcumin_b_D_Glucuronide_Sodium_Salt	-8	ILE A:27, ILE A:437, LYS A:383, ARG A:385, GLN A:439

2.4 Admet Profiling

DeepPK predictions were extracted for the six curcumin analogues that displayed the most favourable docking energies: curcumin bicyclopentadione, perfluoro-curcumin, curcumin 4′-O-β-D-gentiobioside, the methoxy-benzylidene derivative, curcumin diglucoside, and the sodium salt of curcumin β-D-glucuronide. The ADMET properties of the derived phytochemicals targeting the receptors are presented in (Supplementary Tables S2). Across the analogues, DeepPK classified every molecule as a non-inhibitor of the major cytochrome P450 isoforms 1A2, 2C19, 2C9, and 2D6, suggesting a low risk of metabolic drug–drug interactions via these pathways. Toxicological indicators were largely favorable. All six candidates scored as non-mutagenic in the Ames test model, non-carcinogenic in the long-term rodent assay surrogate, and safe concerning hERG channel blockade, pointing to a minimal predicted risk of genotoxicity or oncogenicity.

Therefore, curcumin bicyclopentadione emerges with the most balanced ADMET profile, thereby complementing its superior docking score. This study demonstrated that ADMET profiling indicated all selected compounds showed no adverse effects on absorption, which is a crucial factor for the viability of drugs. Furthermore, the comprehensive pharmacokinetic and toxicity findings were positive, revealing no notable safety issues detected. The results indicate that the candidate compounds exhibit strong ADMET properties, highlighting their promise as suitable therapeutic options for subsequent preclinical advancement. By demonstrating both effective pharmacokinetics and minimal toxicity, curcumin bicyclopentadione stands out as the lead scaffold for biochemical validation and medicinal chemistry optimisation.

2.5 Molecular Dynamics Simulations

For a better understanding of the molecular insights that are involved in the ligand-receptor binding of the top six ligands with the receptor, a 100-ns molecular dynamics simulation was run in GROMACS.

Among the six 100-ns GROMACS trajectories, Curcumin Bicyclopentadione (complex 1) displays the clearest hallmarks of a well-defined ligand–receptor complex (Fig. 4). Its backbone RMSD rises sharply during the first 5 ns and then stabilises in a narrow 0.60–0.75 nm band (Fig. 4B), while the radius of gyration (Rg) contracts from ≈ 2.60 nm to 2.40 nm (Fig. 4C) and undergoes only a modest, reversible expansion thereafter; behaviour consistent with native-like packing rather than global unfolding. Solvent-accessible surface area (SASA) fluctuates around 265 Å with a mild upward drift in the final quarter of the run, mirroring the breathing motions seen in the Rg (Fig. 4A). Crucially, the ligand maintains two to three hydrogen bonds for most frames, and the per-residue RMSF profile is subdued (< 0.25 nm) across the catalytic core, indicating a stable, productive binding pose (Fig. 4E).

Perfluoro-curcumin (complex 2) exhibits a comparably well-damped RMSD plateau around 0.75 nm, alongside a gradual contraction in Rg to approximately 2.40 nm. Additionally, there is a downward trend observed in both SASA and hydrogen-bond scatter, indicating a progressively tighter packing around a consistently buried ligand.

Curcumin 4′-O-β-D-gentiobioside (complex 3) and 4-(4-Hydroxy-3-methoxybenzylidene)-1,7-bis(4-hydroxy-3-methoxyphenyl)hepta-1,6-diene-3,5-dione (complex 4) are markedly less coherent: both exhibit large-amplitude Rg excursions (> 2.70 nm), sustained RMSD values approaching or exceeding 1 nm, and a progressive loss of hydrogen-bond occupancy after ~ 40 ns, pointing to partial pocket rearrangement or incipient ligand egress.

Curcumin diglucoside (complex 5) resembles perfluoro-curcumin in overall stability, with a monotonic Rg decline, a stable RMSD plateau (~ 0.65 nm), and consistent 2–4 hydrogen bonds, accompanied by a stronger SASA reduction that hints at deeper pose within the binding pocket. Ultimately, Curcumin-β-D-glucuronide sodium salt (complex 6) exhibits rapid stabilisation in terms of RMSD, yet demonstrates a late-stage increase in Rg and a corresponding rebound in SASA, alongside a decrease in hydrogen bonds—indicative of pocket reopening rather than complete destabilisation. The MD simulations of complexes 2–6 can be viewed in the Supplementary Figs. 1–5.

Taken together, these simulations single out Curcumin Bicyclopentadione (and, to a lesser extent, perfluoro-curcumin and Curcumin diglucoside) as the most structurally robust candidates. In contrast, Curcumin 4′-O-β-D-gentiobioside and the extended bis-vanillylidene derivative require careful consideration due to their significant global fluctuations and diminished intermolecular interactions, whereas the glucuronide conjugate holds a middle ground, maintaining overall stability but displaying late flexibility that could influence binding energetics.

3. DISCUSSION

Insulin resistance in metabolic syndrome and related disorders occurs mainly because excess lipid metabolites activate protein phosphatase 2A (PP2A). Hyperactivity of PP2A dephosphorylates the Akt node, attenuating insulin-stimulated glucose transport. Thus, interventions targeting the PP2A/Akt axis can enhance insulin sensitivity [23]. Thereforecurrent *in silico* study evaluates curcumin compounds that may inhibit PP2A by binding its regulatory subunit PPP2R5B, a critical facilitator of Akt dephosphorylation.

Naturally occurring phytochemicals serve as valuable sources for the development of novel treatment strategies for various metabolic diseases. Owing to their minimal side effects and notable efficacy, these phytochemicals are widely favored choices for ameliorating metabolic disorders [24]. Curcumin, renowned for its wide range of

therapeutic properties, holds significant potential as an agent for enhancing metabolic parameters [25]. Using the keyword “curcumin,” we identified approximately 85 compounds from the PubChem database. Curcumin, a naturally occurring compound in turmeric, has garnered significant attention for its extensive pharmacological properties, particularly its therapeutic role in combating insulin resistance. In addition to its well-documented anti-inflammatory and anticancer effects, curcumin has shown promising potential in enhancing insulin sensitivity and regulating glucose metabolism. By modulating diverse signaling pathways and reducing oxidative stress, curcumin improves insulin-receptor function and facilitates cellular glucose uptake. These mechanisms contribute to its effectiveness in managing insulin resistance, offering a natural and potent alternative for preventing and treating conditions such as type 2 diabetes and metabolic syndrome [15, 26]. However, its specific interactions with cellular proteins have not been fully elucidated. The serine/threonine-protein phosphatase 2A 56 kDa regulatory subunit beta isoform plays a crucial role in regulating various cellular processes, including cell cycle progression, apoptosis, and cellular signaling [8, 13].

The binding interactions between these compounds and the protein were meticulously characterized using molecular docking studies. This computational analysis identified the key residues at the binding interface and elucidated the possible mechanisms of inhibition (subjected to experimental investigation). The results indicated that the top-ranked curcumin compounds, such as curcumin-bicyclopentadione exhibited significantly higher binding affinities with the serine/threonine-protein phosphatase 2A 56 kDa regulatory subunit beta isoform. This enhanced binding affinity suggests promising pharmacological activity and therapeutic efficacy, and can be particularly useful in managing insulin resistance. These findings corroborate the hypothesis that ligands engaging both basic patches of PPP2R5B yield the most favorable interaction energies and therefore represent the most promising scaffolds for experimental optimization. They also highlight the potential of curcumin compounds as effective agents for the treatment of conditions such as type 2 diabetes, emphasizing their role in improving insulin sensitivity and regulating glucose metabolism.

The static docking outcomes were reinforced by 100-ns molecular-dynamics simulations. Curcumin-bicyclopentadione maintained a narrowly fluctuating backbone RMSD and a stable hydrogen-bond network throughout the trajectory, while its radius of gyration contracted, indicating compaction of the complex and absence of global unfolding. Perfluoro-curcumin and curcumin diglucoside showed similar, though slightly less pronounced, stabilisation, whereas gentiobioside and the bis-vanillylidene derivative underwent late-stage pocket breathing and partial ligand egress, underscoring the relevance of scaffold rigidity and limited rotatable bonds for sustained inhibition. Together, these data suggest that bicyclic modifications may pre-organize the β-diketone

core into an energetically privileged conformation that resists displacement by solvent fluctuations.

The *in silico* drug screening of curcumin delivers a first-pass filter that prioritizes molecules that are likely to succeed in a downstream assay [27, 28]. The ADMET analysis demonstrated that all six lead candidates are predicted non-inhibitors of the major CYP450 isoforms, non-mutagenic in Ames simulations, non-carcinogenic in rodent surrogates, and free of hERG channel blockade liabilities, implying a favourable drug-drug interaction and cardiotoxicity profile. The findings from the ADMET analysis indicated that the chosen compounds displayed advantageous pharmacokinetic characteristics, suggesting they have the potential to be effectively absorbed, properly distributed within the body, efficiently metabolized, and show low toxicity levels. These attributes are crucial for any substance evaluated for medicinal application [29, 30].Notably, curcumin-bicyclopentadione combines the highest binding affinity with the most balanced ADMET characteristics, marking it as a prime candidate for cell-based validation.

Based on docking, dynamics, and pharmacokinetic evaluations, it is concluded that the leading phytochemicals can inhibit PPP2R5B by occupying its LxxIxE-recognition cleft and shielding catalytic residues from substrate access. By effectively targeting this protein, these molecules may re-sensitize Akt and restore insulin-stimulated glucose uptake, so they could disrupt the pathological cascades that underlie insulin resistance and possibly mitigate downstream sequelae such as hepatic gluconeogenesis and adipose inflammation (shown in Fig. 5). Although *PPP2R5B* has also been implicated in oncogenic signaling, the comparatively benign ADMET predictions for the curcumin scaffolds raise the prospect of dual-utility nutraceuticals capable of moderating both metabolic and neoplastic pathways [8, 13].

Nevertheless, these insights derive solely from computational predictions. Future work should include surface-plasmon-resonance and isothermal-titration-calorimetry assays to quantify binding kinetics, followed by CRISPR-mediated PPP2R5B knock-out studies in insulin-resistant adipocytes to benchmark biochemical efficacy against genetic abrogation. Acute and chronic dosing experiments in rodent models of diet-induced obesity will be essential to verify bioavailability, confirm modulation of hepatic gluconeogenic gene expression, and monitor off-target phosphatase inhibition. Parallel medicinal-chemistry campaigns may explore fluorination or bicyclic locking to enhance metabolic stability and circumvent the well-known low oral bioavailability of native curcumin [31].

In conclusion, the integrated in-silico pipeline identifies curcumin-bicyclopentadione as a structurally robust, pharmacokinetically acceptable, and mechanistically plausible inhibitor of PPP2R5B. By bridging natural-product chemistry with contemporary computational pharmacology, the present study delivers a rationale for repurposing

curcuminoids as scaffolds for metabolic-disease therapeutics, thereby contributing a novel dimension to the expanding repertoire of PP2A-targeted interventions.

4. Methodology

The methodology adopted for the identification of curcumin-derived phytochemicals capable of inhibiting PPP2R5B was spanned across four phases of a comprehensive set of computational steps that fulfilled the *in silico* nature of our study. The step-wise methodology is illustrated in Fig. 6.

4.1 Structure retrieval and refinement

The protein-coding *PPP2R5B* gene from *Homo sapiens* was retrieved on the basis of available literature reported by Beg et al. in 2016, which refers to its role as a negative regulator of Akt phosphorylation, significantly contributing to insulin resistance-induced hyperinsulinemia in adipocytes [13]. The *PPP2R5B* (B56β) protein sequence was retrieved from Uniprot under the ID: Q15173 (available at https://www.uniprot.org/uniprotkb/Q15173/entry) [32]. The corresponding 3D structure of the protein was predicted using the default parameters in the SWISS-MODEL (http://swissmodel.expasy.org) server, the most widely used free web-based automated modeling facility [33]. The predicted structure was then refined using GalaxyRefine [34], and later the structure was validated through the PROCHECK [35] program's stereochemical assessment using an ERRAT quality factor and Ramachandran plot.

4.2 Ligand library preparation of curcumin analogues

The preliminary details of the curcumin compounds were obtained from the literature [36, 37]. Subsequently, a 3D structure-based library containing compounds reported from curcumin and its derivatives was generated. The structures of the selected compounds were retrieved from PubChem (https://pubchem.ncbi.nlm.nih.gov). Following visual examination of each 3D compound, the structures were initially downloaded in the Structure Data Format (SDF) and then converted into the Protein Data Bank (PDB) format using Discovery studio Visualizer (https://www.3ds.com/products/biovia/discovery-studio/visualization) [38]. The analogues were then prepared for molecular docking and converted to PDBQT format using AutoDockTools (available at https://autodocksuite.scripps.edu/adt/). To identify stable conformations, energy minimization of the compounds was performed to ascertain a configuration space in which all forces on the atoms were balanced.

4.3 Docking preparation and analysis

4.3.1 Receptor preparation and prediction of receptor binding pockets

The receptor was prepared for molecular docking by employing AutoDockTools. The water molecules were eliminated, while polar hydrogen and Kollman charges were added to the receptor for an efficient docking process. The prepared structure was then saved in a PDBQT format. The receptor's binding pockets were predicted using Fpocket, an open-source platform for ligand pocket detection [39]. Before docking, the coordinates of these pockets were subsequently utilized to create an output grid dimensions file by employing the AutoDockTools to configure all top-ranked compounds to completely cover the binding residues within the 3D energy-minimized model of the human *PPP2R5B* gene. The corresponding formats of the ligands (curcumin analogues) and the *PPP2R5B* gene for this analysis were also in the form of PDBQT files.

4.3.2 Molecular Docking

The ligand library of 85 phytochemicals was docked with the key interacting residues of the *PPP2R5B* protein structure. AutoDock Vina software (version 4.2) was used to analyze the molecular binding interactions between proteins and screened compounds of curcumin [40]. The most favorable binding interactions were estimated using the lowest predicted binding free energy with the best molecular docking simulation pose [41]. The top 6 complexes, based on their binding energies, were selected for further analysis, which included absorption, distribution, metabolism, excretion, and toxicity (ADMET) analysis of ligands and docked complex visualizations. The top 6 docked complexes were further visualized using the Biovia DS Studio Visualizer [38]. Both two-dimensional and three-dimensional interaction diagrams were prepared.

4.4 Pharmacokinetic and toxicity prediction through ADMET Analysis

The ADMET approach was used for the top-ranked compounds, which showed higher binding affinities for the serine/threonine-protein phosphatase 2A 56 kDa regulatory subunit beta isoform (*PPP2R5B*) in computational analysis. *In silico* pharmacokinetic and toxicity predictions of the selected compounds were performed using the DeepPK platform https://biosig.lab.uq.edu.au/deeppk/) to assess the ADMET properties [42]. Each physicochemical property was assessed by submitting the canonical SMILE format of the individual compound.

4.5 Molecular Dynamics Simulation

The stability of the docked complexes was analyzed using a 100-ns Molecular Dynamics simulation research experiment. The GROMACS program, version 2021.2, was utilized for

the molecular dynamics simulations of the docked complexes [43, 44]. The Optimised Potential for Liquid Simulations (OPLS) force field was employed, and the structure was positioned within a cubic unit cell at a distance of 1.0 nm from the box edge. The Simple Point Charge (SPC) water model was employed for solvation, followed by the neutralization of the system through the substitution of solvent molecules with Cl- ions. A maximum of 50,000 steps of energy minimization were conducted on the previously predicted models utilizing a conjugate gradient algorithm, followed by steepest descent minimization. Following energy minimization, the system underwent equilibration via position-restrained simulation within an NVT ensemble (constant Number of particles, Volume, and Temperature) for 100 picoseconds, achieving temperature stabilization at 300 K using the Berendsen thermostat. A comparative examination of structural deviations, including root mean square deviation (RMSD), root mean square fluctuation (RMSF), radius of gyration (Rg), and hydrogen bonds, was conducted using GROMACS utility packages.

Declarations

Author contributions

Dr. Sadaf and Dr. Aneela conceived and planned the idea, verified the analytical methods, investigated and supervised the findings of the work, proofread the manuscript, and formulated a conceptual framework. Maaz Waseem performed the analytical methods and proofread the manuscript. Saifullah Khan performed various analysis such as docking and simulation, while Zainab Kamran was part of the write-up and proofreading of the manuscript. Maham yamin conducted the analysis of our data along with some of the write-up of this manuscript.

Data availability statement

All relevant data will be made available to the editors upon request. You can contact the corresponding author Dr. Aneela Javed (javedaneela19@asab.nust.edu.pk) for any data related to this study.

Additional Information

Competing interests
The author(s) declare no competing interests.

Funding Declaration
This study received no funding.

References

1. Clemente-Suárez, V.J., et al. New insights and potential therapeutic interventions in metabolic diseases. *International journal of molecular sciences*, 2023. **24**(13): p. 10672.
2. Wu, X., et al. Targeting protein modifications in metabolic diseases: molecular mechanisms and targeted therapies. *Signal transduction and targeted therapy*, 2023. **8**(1): p. 220.
3. Turner, J., A. Kumar, and C. Koch. The effects of indoor and outdoor temperature on metabolic rate and adipose tissue–the Mississippi perspective on the obesity epidemic. *Reviews in Endocrine and Metabolic Disorders*, 2016. **17**: p. 61-71.
4. Heindel, J.J., et al. Metabolism disrupting chemicals and metabolic disorders. *Reproductive toxicology*, 2017. **68**: p. 3-33.
5. Moin, H., et al. Effectiveness of analog of Humanin in ameliorating streptozotocin-induced diabetic nephropathy in Sprague Dawley rats. *Peptides*, 2023. **165**: p. 171014.
6. Pérez-Martínez, P., et al. Lifestyle recommendations for the prevention and management of metabolic syndrome: an international panel recommendation. *Nutrition reviews*, 2017. **75**(5): p. 307-326.
7. Galbo, T., G.S. Olsen, B. Quistorff, and E. Nishimura. Free fatty acid-induced PP2A hyperactivity selectively impairs hepatic insulin action on glucose metabolism. *PloS one*, 2011. **6**(11): p. e27424.
8. Chen, L., et al. Protein phosphatase 2A regulates cytotoxicity and drug resistance by dephosphorylating AHR and MDR1. *Journal of Biological Chemistry*, 2022. **298**(5): p. 101918.
9. Yang, R., et al. Functional genetic polymorphisms in PP2A subunit genes confer increased risks of lung cancer in southern and eastern Chinese. *PLoS One*, 2013. **8**(10): p. e77285.
10. Jun, H.S., K. Hwang, Y. Kim, and T. Park. High-fat diet alters PP2A, TC10, and CIP4 expression in visceral adipose tissue of rats. *Obesity*, 2008. **16**(6): p. 1226-1231.
11. Galbo, T., et al. PP2A inhibition results in hepatic insulin resistance despite Akt2 activation. *Aging (Albany NY)*, 2013. **5**(10): p. 770.
12. Rodgers, J.T., R.O. Vogel, and P. Puigserver. Clk2 and B56β mediate insulin-regulated assembly of the PP2A phosphatase holoenzyme complex on Akt. *Molecular cell*, 2011. **41**(4): p. 471-479.
13. Beg, M., et al. PPP2R5B, a regulatory subunit of PP2A, contributes to adipocyte insulin resistance. *Molecular and cellular endocrinology*, 2016. **437**: p. 97-107.
14. Wang, Y.-Y., A.C. Hung, S. Lo, and S.-S.F. Yuan. Adipocytokines visfatin and resistin in breast cancer: Clinical relevance, biological mechanisms, and therapeutic potential. *Cancer letters*, 2021. **498**: p. 229-239.

15. Sedighiyan, M., et al. The effects of nano-curcumin supplementation on adipokines levels in obese and overweight patients with migraine: a double blind clinical trial study. *BMC Research Notes*, 2022. **15**(1): p. 189.
16. Dehzad, M.J., H. Ghalandari, M.R. Amini, and M. Askarpour. Effects of curcumin/turmeric supplementation on lipid profile: A GRADE-assessed systematic review and dose–response meta-analysis of randomized controlled trials. *Complementary Therapies in Medicine*, 2023. **75**: p. 102955.
17. Marton, L.T., et al. The effects of curcumin on diabetes mellitus: a systematic review. *Frontiers in endocrinology*, 2021. **12**: p. 669448.
18. Choi, J.-W., et al. Reduction in prevalence of hypertension and blood heavy metals among curry-consumed Korean. *The Tohoku Journal of Experimental Medicine*, 2018. **244**(3): p. 219-229.
19. Moetlediwa, M.T., et al. Evaluating the therapeutic potential of Curcumin and synthetic Derivatives: a computational approach to anti-obesity treatments. *International Journal of Molecular Sciences*, 2024. **25**(5): p. 2603.
20. Latif, R., S. Mumtaz, M.H. Al Sheikh, S. Chathoth, and S.N. Al Naimi. Effects of turmeric on cardiovascular risk factors, mental health, and serum homocysteine in overweight, obese females. *Altern. Ther. Health Med*, 2021. **27**(S1): p. 114-119.
21. Han, X., et al. Curcumin inhibits protein phosphatases 2A and 5, leading to activation of mitogen-activated protein kinases and death in tumor cells. *Carcinogenesis*, 2012. **33**(4): p. 868-875.
22. Cocorocchio, M., et al. Curcumin and derivatives function through protein phosphatase 2A and presenilin orthologues in Dictyostelium discoideum. *Disease Models & Mechanisms*, 2018. **11**(1): p. dmm032375.
23. Obanda, D.N., D. Ribnicky, Y. Yu, J. Stephens, and W.T. Cefalu. An extract of Urtica dioica L. mitigates obesity induced insulin resistance in mice skeletal muscle via protein phosphatase 2A (PP2A). *Scientific reports*, 2016. **6**(1): p. 22222.
24. Luo, Y., et al. Phytochemicals for the treatment of metabolic diseases: Evidence from clinical studies. *Biomedicine & Pharmacotherapy*, 2023. **165**: p. 115274.
25. Qiu, L., et al. Effects of dietary polyphenol curcumin supplementation on metabolic, inflammatory, and oxidative stress indices in patients with metabolic syndrome: a systematic review and meta-analysis of randomized controlled trials. *Frontiers in endocrinology*, 2023. **14**: p. 1216708.
26. Zhang, D.-w., M. Fu, S.-H. Gao, and J.-L. Liu. Curcumin and diabetes: a systematic review. *Evidence-Based Complementary and Alternative Medicine*, 2013. **2013**(1): p. 636053.
27. Bruno, A., G. Costantino, L. Sartori, and M. Radi. The in silico drug discovery toolbox: applications in lead discovery and optimization. *Current Medicinal Chemistry*, 2019.

26(21): p. 3838-3873.

28. Shaker, B., S. Ahmad, J. Lee, C. Jung, and D. Na. In silico methods and tools for drug discovery*. Computers in biology and medicine*, 2021. **137**: p. 104851.
29. Shweta, M. and D. Rashmi. In-vitro ADME studies of TUG-891, a GPR-120 inhibitor using Swiss ADME predictor*. Journal of drug delivery and therapeutics*, 2019. **9**(2-S): p. 266-369.
30. Aloufi, B., F.M. Alshabrmi, N. Sreeharsha, and A. Rehman. Exploring therapeutic targets and drug candidates for obesity: a combined network pharmacology, bioinformatics approach*. Journal of Biomolecular Structure and Dynamics*, 2024. **42**(21): p. 11879-11900.
31. Caron, G. and G. Ermondi, *Molecular descriptors for polarity: the need for going beyond polar surface area*. 2016, Taylor & Francis. p. 2013-2016.
32. Consortium, U. UniProt: a worldwide hub of protein knowledge*. Nucleic acids research*, 2019. **47**(D1): p. D506-D515.
33. Schwede, T., J. Kopp, N. Guex, and M.C. Peitsch. SWISS-MODEL: an automated protein homology-modeling server*. Nucleic acids research*, 2003. **31**(13): p. 3381-3385.
34. Heo, L., H. Park, and C. Seok. GalaxyRefine: Protein structure refinement driven by side-chain repacking*. Nucleic acids research*, 2013. **41**(W1): p. W384-W388.
35. Laskowski, R., M. MacArthur, and J. Thornton. PROCHECK: validation of protein-structure coordinates*.* 2006.
36. Stanić, Z. Curcumin, a compound from natural sources, a true scientific challenge–a review*. Plant Foods for Human Nutrition*, 2017. **72**: p. 1-12.
37. Noureddin, S.A., R.M. El-Shishtawy, and K.O. Al-Footy. Curcumin analogues and their hybrid molecules as multifunctional drugs*. European journal of medicinal chemistry*, 2019. **182**: p. 111631.
38. Visualizer, D. Discovery studio visualizer. 2*. Accelrys software inc*, 2005.
39. Le Guilloux, V., P. Schmidtke, and P. Tuffery. Fpocket: an open source platform for ligand pocket detection*. BMC bioinformatics*, 2009. **10**: p. 1-11.
40. Xue, Q., et al. Evaluation of the binding performance of flavonoids to estrogen receptor alpha by Autodock, Autodock Vina and Surflex-Dock*. Ecotoxicology and Environmental Safety*, 2022. **233**: p. 113323.
41. Terefe, E.M. and A. Ghosh. Molecular docking, validation, dynamics simulations, and pharmacokinetic prediction of phytochemicals isolated from Croton dichogamus against the HIV-1 reverse transcriptase*. Bioinformatics and biology insights*, 2022. **16**: p. 11779322221125605.

42. Myung, Y., A.G. de Sá, and D.B. Ascher. Deep-PK: deep learning for small molecule pharmacokinetic and toxicity prediction. *Nucleic acids research*, 2024. **52**(W1): p. W469-W475.
43. Hess, B., L.E. van der Spoel, and E. Lindahl. GROMACS Groningen machine for chemical simulations. *User Manual. Version*, 2011. **4**(4).
44. Abraham, M., D. Van Der Spoel, E. Lindahl, and B. Hess. GROMACS user manual version 5.0. 4. *The GROMACS Development Team at the Royal Instituta of Technology and Uppsala University, Sweden*, 2014.

Figures

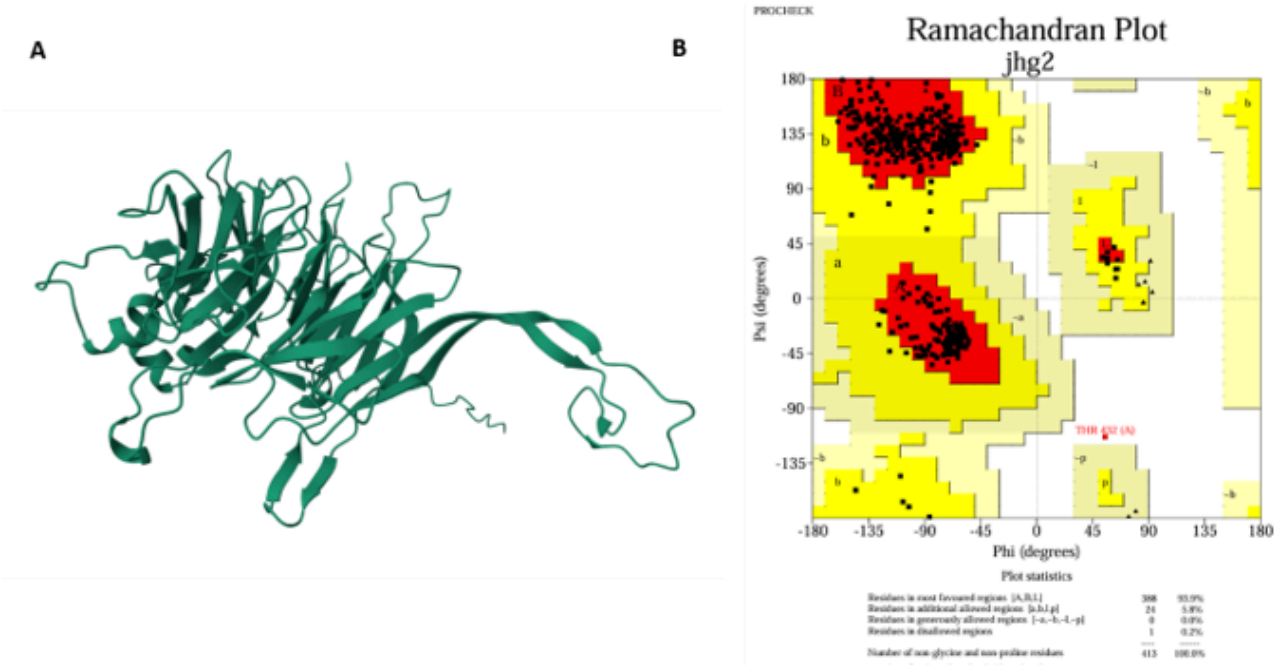


Figure 1

Homology model generation and validation of PPP2R5B. A) Refined 3D structure of PP2RB5 **B)** Validation of the 3D structure through a Ramachandran plot

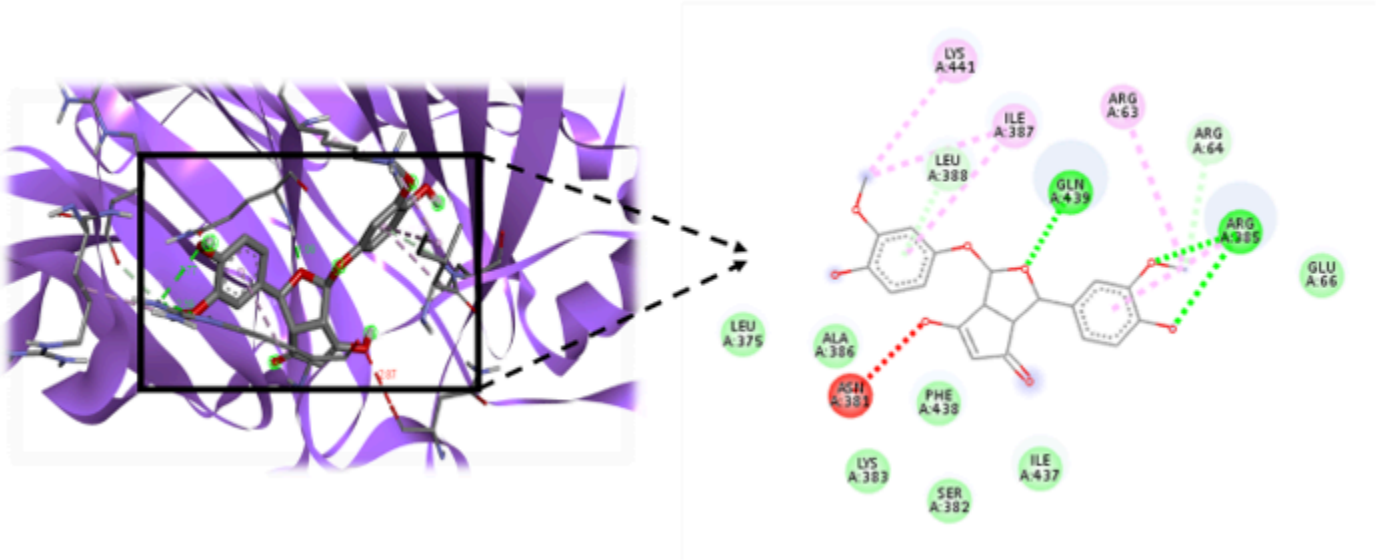


Figure 2

Binding pose of curcumin-bicyclopentadione within the PPP2R5B pocket.

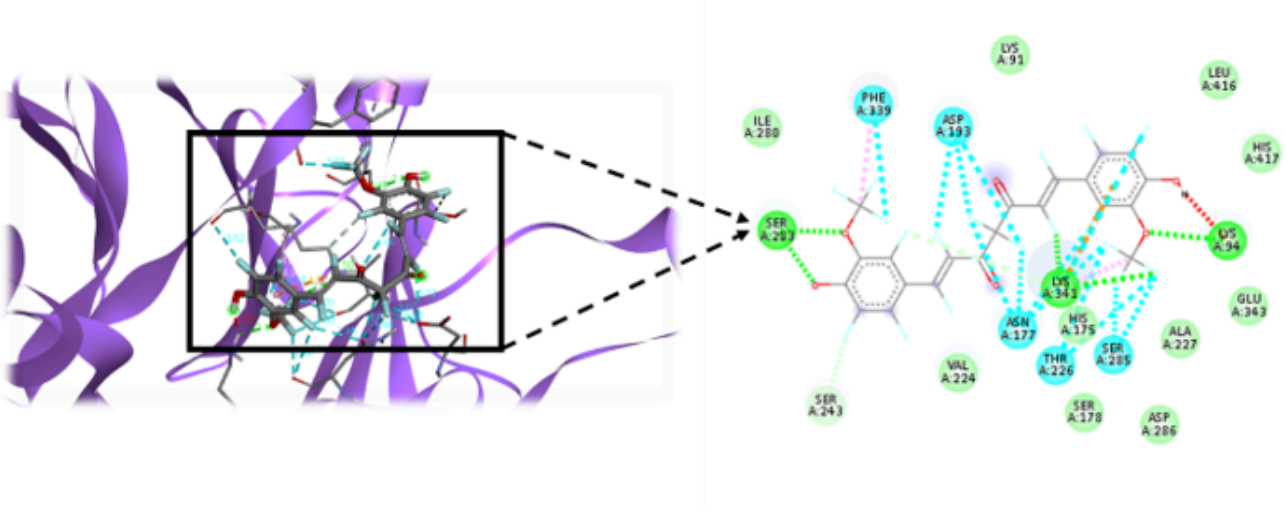


Figure 3

Docking configuration of perfluoro-curcumin, the second-ranked ligand. The 3D and 2D structures of the ligand-receptor complex of Perfluoro-curcumin

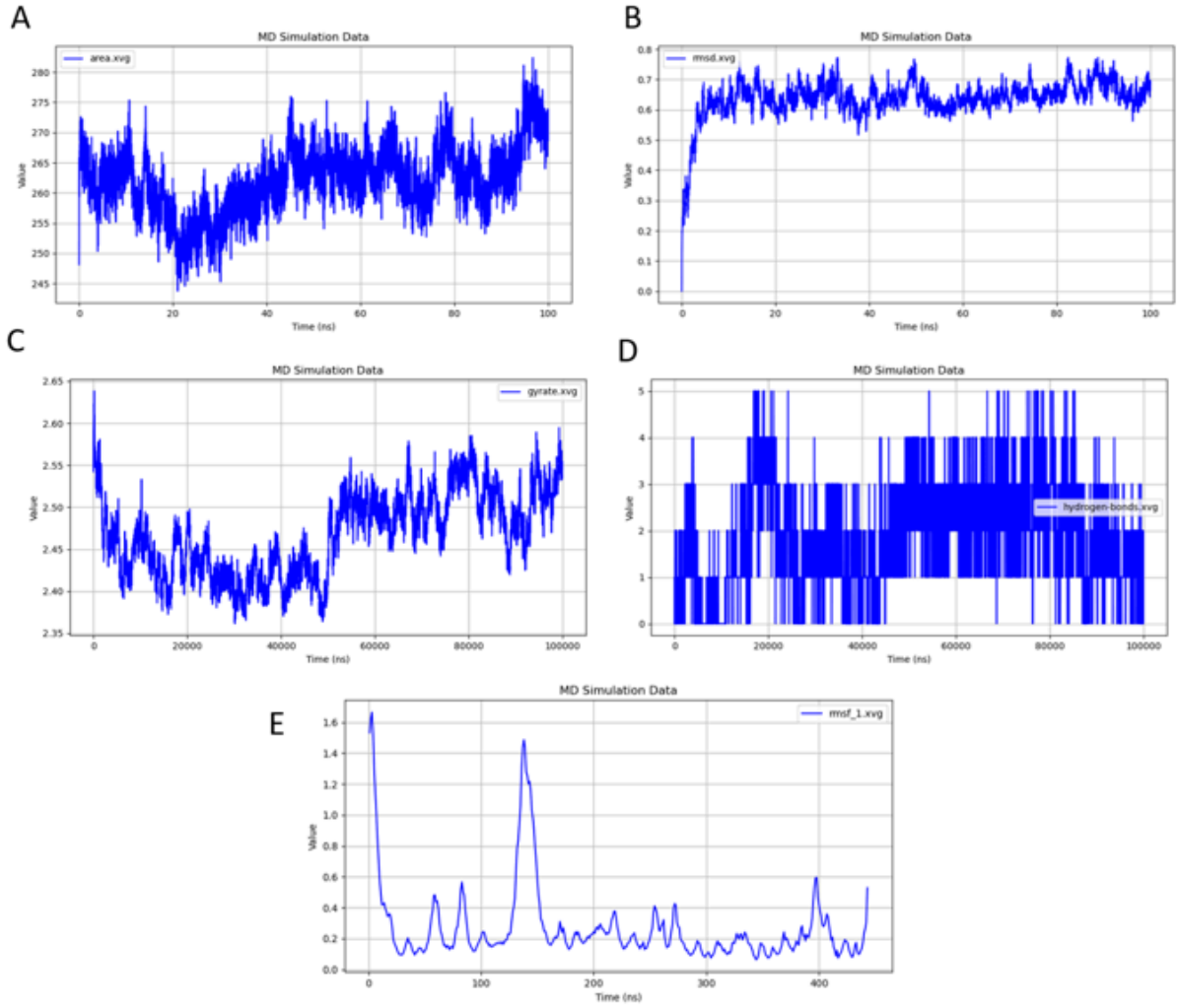


Figure 4

Molecular-dynamics stability of the PPP2R5B–curcumin-bicyclopentadione complex over 100 ns. Analysis of the top-ranked complex Curcumin Bicyclopentadione with it's receptor A) SASA analysis B) RMSD C) Radius of gyration analysis D) Hydrogen bonds E) RMSF analysis. The analysis indicates a stable, productive binding pose.

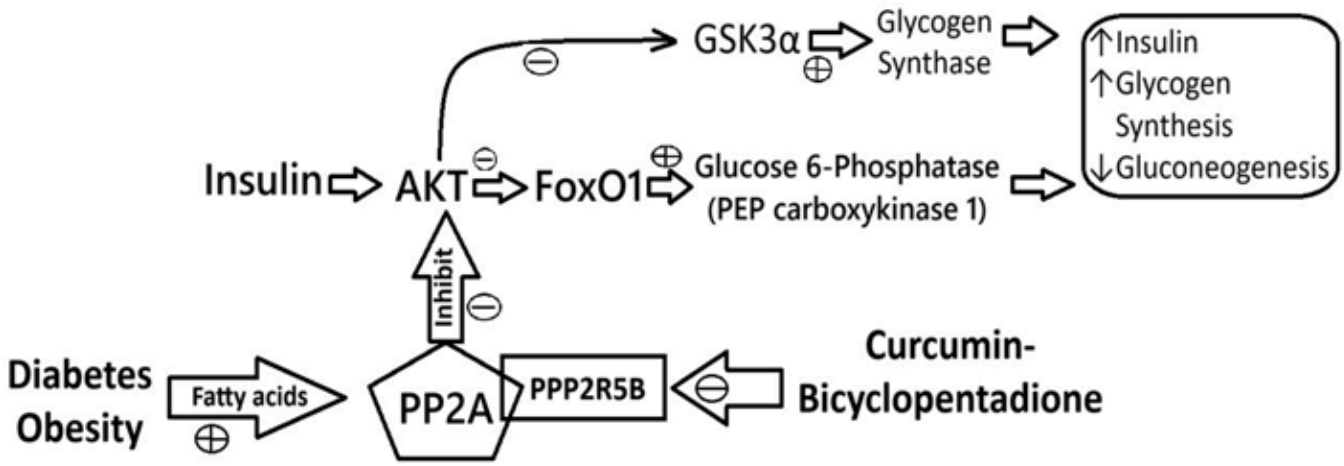


Figure 5

Shows insilico identified curcumin-bicyclopentadione inhibitor of PPP2R5B. Under normal Physiological conditions insulin stimulates Akt which inhibits Fox01 and GSK3a stimulating Glucose 6-phosphatase and glycogen synthase enzymes, respectively. This enhances insulin sensitivity transferring GLUT-4 to the membrane, promoting glycogen synthesis and reducing gluconeogenesis. Excessive fatty acids In diabetes, obesity and metabolic syndrome, directly stimulates PP2A which inhibits AKT and its insulin sensitizing effects. Curcumin - bicyclopentadione can potentially inhibit PPP2R5B thereby enhancing the insulin sensitivity through Akt pathway.

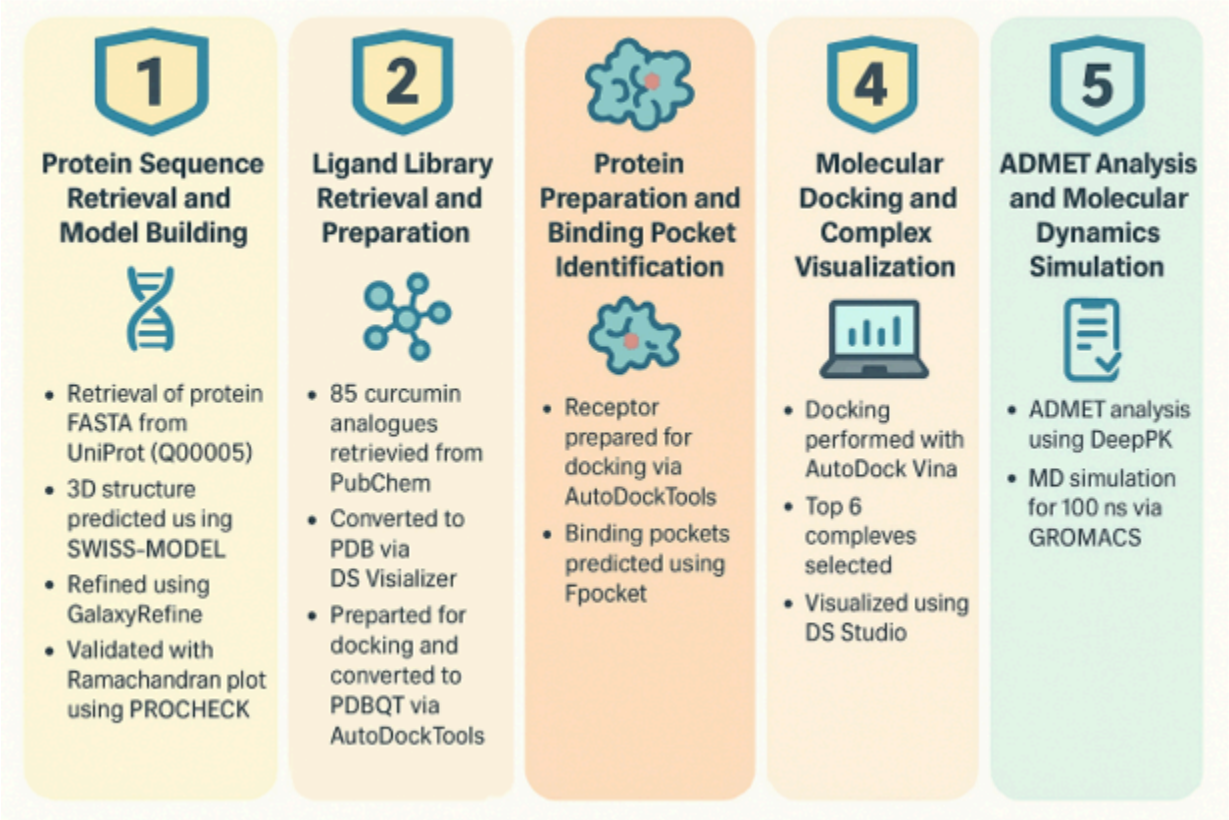


Figure 6

Step-wise research methodology of the current study.

Supplementary Files

This is a list of supplementary files associated with this preprint. Click to download.

- Supplementaryfigures.pdf
- SupplementaryTables.xlsx